Journal of Medical and Biological Engineering

16-Channel Surface Coil for 13C-Hyperpolarized Spectroscopic Imaging of Cardiac Metabolism in Pig Heart

--Manuscript Draft--

Manuscript Number:	JMBE-D-15-00008R2
Full Title:	16-Channel Surface Coil for 13C-Hyperpolarized Spectroscopic Imaging of Cardiac Metabolism in Pig Heart
Article Type:	Original Article
Funding Information:	
Abstract:	Purpose: Magnetic resonance spectroscopy of hyperpolarized 13C pyruvate and its metabolites in large animal models is a powerful tool for assessing cardiac metabolism in patho-physiological conditions. In 13C studies the Signal-to-Noise Ratio (SNR) could be crucial, to overcome intrinsic data quality limitation due to the low molar concentration of certain metabolites as well as the low flux of conversion. On the other hand, since 13C-MRS is essentially a semi-quantitative technique, the SNR among the spectra acquired in different myocardial segments should be homogeneous. MR coil design plays an important role in achieving both targets. Materials and Methods: In this study, a receive 16-channels surface coil was designed for 13C hyperpolarized studies of pig heart with a clinical 3T scanner. The coil performances were characterized by phantom experiments, and compared with a birdcage coil used in transmit/receive mode. Segmental signal distribution in the left ventricle (LV) was assessed by experiments on six healthy mini pigs. Results: The proposed coil showed a significant increase in SNR in the LV wall close to the coil surface with respect to the birdcage but also a significant segmental inhomogeneity. Conclusion: The use of the 16-channel coil would be recommended in studies of septal and anterior LV walls.
Corresponding Author:	Vincenzo Positano, MSc ITALY
Corresponding Author Secondary Information:	
Corresponding Author's Institution:	
Corresponding Author's Secondary Institution:	
First Author:	Francesca Frijia, MSc
First Author Secondary Information:	
Order of Authors:	Francesca Frijia, MSc
	Ulrich Koellisch, PhD
	Maria Filomena Santarelli, PhD
	Giulio Giovannetti, PhD
	Titus Lanz, PhD
	Alessandra Flori, PhD
	Markus Durst, PhD
	Giovanni Donato Aquaro, MD
	Rolf F Schulte, PhD
	Daniele De Marchi, RT
	Vincenzo Lionetti, MD

	Jan H Ardenkjaer-Larsen, PhD
	Luigi Landini, PhD
	Luca Menichetti, PhD
	Vincenzo Positano, MSc
Order of Authors Secondary Information:	
Author Comments:	Dear Editor, enclosed the edited version of the manuscript "16-channels surface coil for hyperpolarized 13C studies of pig heart" for pubblication on JMBE Journal. The paper was previously submitted (JMBE-D-15-00008R1) and accepted with request of final editing. With the Best Regards, Vincenzo Positano Fondazione G Monasterio Via Moruzzi, 1 56124, PISA, ITALY Phone: +39 050 3152613 Fax: +39 050 3153535 e-mail: positano@ftgm.it
Response to Reviewers:	The requested correction were done on the revised manuscript.

16-Channel Surface Coil for ^{13}C-Hyperpolarized Spectroscopic Imaging of Cardiac Metabolism in Pig Heart

Francesca Frijia[1], Maria Filomena Santarelli[2,1], Ulrich Koellisch[3], Giulio Giovannetti[2,1], Titus Lanz[4], Alessandra Flori[1], Markus Durst[3], Giovanni Donato Aquaro[1], Rolf F. Schulte[5], Daniele De Marchi[1], Vincenzo Lionetti[6], Jan H Ardenkjaer-Larsen[7,8], Luigi Landini[1,9], Luca Menichetti[2,1], Vincenzo Positano[1].

[1] Fondazione G. Monasterio CNR-Regione Toscana, 56124, Pisa, Italy

[2] Institute of Clinical Physiology, National Research Council, 56124, Pisa, Italy

[3] Technische Universität München, Institute of Medical Engineering, 80333, Munich, Germany

[4] Rapid Biomedical GmbH, 97222, Rimpar, Germany

[5] GE Global Research, 80333, Munich, Germany

[6] Laboratory of Medical Science, Institute of Life Sciences, Scuola Superiore Sant'Anna, 56126, Pisa, Italy

[7] Department of Electrical Engineering, Technical University of Denmark, 2800 Kgs, Lyngby, Denmark

[8] GE Healthcare, 2605, Broendby, Denmark

[9] Department of Information Engineering, University of Pisa, 56126, Pisa, Italy

*Corresponding author:

Vincenzo Positano, MSc

Fondazione CNR Regione Toscana “G. Monasterio”

Via Moruzzi, 1, 56124, PISA, ITALY

Phone: +39 050 3152613

Fax: +39 050 3153535

e-mail: positano@ftgm.it

Running title: 16-channel surface coil for 13C spectroscopy

Word count: 3400

Abstract

Purpose: Magnetic resonance spectroscopy of hyperpolarized ^{13}C pyruvate and its metabolites in large animal models is a powerful tool for assessing cardiac metabolism in patho-physiological conditions. In ^{13}C studies the Signal-to-Noise Ratio (SNR) could be crucial, to overcome intrinsic data quality limitation due to the low molar concentration of certain metabolites as well as the low flux of conversion. On the other hand, since ^{13}C-MRS is essentially a semi-quantitative technique, the SNR among the spectra acquired in different myocardial segments should be homogeneous. MR coil design plays an important role in achieving both targets.

Materials and Methods: In this study, a receive 16-channels surface coil was designed for ^{13}C hyperpolarized studies of pig heart with a clinical 3T scanner. The coil performances were characterized by phantom experiments, and compared with a birdcage coil used in transmit/receive mode. Segmental signal distribution in the left ventricle (LV) was assessed by experiments on six healthy mini pigs.

Results: The proposed coil showed a significant increase in SNR in the LV wall close to the coil surface with respect to the birdcage but also a significant segmental inhomogeneity.

Conclusion: The use of the 16-channel coil would be recommended in studies of septal and anterior LV walls.

Keywords: Hyperpolarized ^{13}C; Magnetic Resonance Imaging; pig model; heart metabolism; RF coils; Dynamic Nuclear Polarization (DNP); ^{13}C-pyruvate

Abbreviations used: **FOV**, field of view; **LV**, left ventricle; **AHA**, American Heart Association; **TE**, echo time; **TR**, repetition time

1 Introduction

^{13}C hyperpolarization through dissolution-DNP has recently been introduced in the field of Magnetic Resonance Spectroscopy (MRS) and Chemical Shift Imaging (CSI) to significantly increase the available SNR [1] for studies in vivo. However, in vivo MRS and CSI studies with hyperpolarized ^{13}C-labeled tracers require the set-up of sophisticated approaches for the acquisition of the spectroscopic signal, including suitable time- and spatially-resolved RF sequences and dedicated coils.

The design and development of dedicated RF coils are necessary constraints for maximizing SNR in hyperpolarized MR experiments. In fact, high SNR is desirable for the evaluation of the *in vivo* kinetic of metabolites, after the injection of hyperpolarized ^{13}C-labelled compounds [2]. In particular, cardiac metabolism assessment with hyperpolarized ^{13}C in pig models requires the design of a dedicated transmit and receive coil operating at the ^{13}C frequency (32.1MHz at 3T), which has to provide the desired field-of-view (FOV) and an optimal SNR. Volume coils are generally used for transmission (TX) due to their homogeneous excitation patterns over a large volume within the coil. Although volume coils can be used for reception (RX) as well, usually surface coils provide the better filling factor and thus the better SNR. The missing B1 homogeneity of the surface coil is no constraint during reception since the B1 profile can be corrected during data reconstruction.

To date, several coil configurations have been implemented and tested for in vivo experiments with MRS of hyperpolarized ^{13}C in different experimental animal models.

In small animal models such as rabbits [3] and mice [4], dual tuned volume $^{1}H/^{13}C$ coils were employed for hyperpolarized ^{13}C studies; to increase the SNR for tumour detection, a ^{13}C surface coil [5] was described. For cardiac studies in large animal models (pigs), ^{13}C volume TX/RX coils were specifically designed [6]. A dedicated ^{13}C TX/RX surface coil for metabolic studies was also proposed including a SNR model [7]. A comparison between a commercial ^{13}C quadrature birdcage coil and a homebuilt ^{13}C circular coil, both designed for hyperpolarized studies of the porcine heart with a clinical 3T scanner, was introduced in [8], and was carried out in terms of sensitivity regions and SNR. Furthermore two RX butterfly coils were presented with different geometries for ^{13}C hyperpolarized studies of pigs [9]; experimental SNR profiles acquired in a phantom highlight the advantage of this configuration over a volume birdcage coil in a wide range of coil-to-voxel distances. Moreover, in [10] the design and implementation of a quadrature surface coil constituted by a circular loop and a butterfly coil, is described; the coil was then tested by acquiring

metabolic maps with hyperpolarized [1–^{13}C]pyruvate injected in vivo in a pig on a 3T clinical scanner. Dominguez-Viqueira et al. [11] demonstrated that by using a dual channel overlapping receive coil it is possible to extend the field of view (FOV) while retaining the SNR performance of a single-element coil. All these studies suggest that joining an appropriate design of RX surface coils with an increased number of channels may enlarge the achievable FOV with stable SNR.

In this study, the performance of a 16-channel RX coil for imaging pyruvate and its metabolites in the whole mini pig heart was investigated. The study also contained phantom tests as in vivo imaging on six healthy mini pigs with a birdcage as TX and the 16-channel-array as RX coil, respectively. Maximal SNR and signal uniformity through the left ventricle (LV) were assessed.

2 Materials and Methods

2.1 Coil design

The receive (RX) coil has an ^{1}H-like flexible array configuration for humans and it is composed of 16 elements resonating at 32.1 MHz (^{13}C frequency at 3T) (Fig. 1(a)) [12].

Each elliptic element has a size of 5 x 8 cm^2 with a conductor width of 2 mm (Fig. 1(b)). Symmetric coupling schemes including cable traps were used for fixed tuning and matching (Fig. 1(c)). Active decoupling was performed by PIN diodes within ^{13}C traps; passive ^{1}H traps including ^{1}H cable traps were used for decoupling resonator and wiring from the ^{1}H body coil. In order to evaluate the potential performance in human applications, all safety mechanisms such as passive PIN diode traps and fuses were included although these mean a lower Q, and thus lower overall SNR. Preamplifier decoupling was performed by transforming the high S11 of the preamplifier input to a high impedance in the coil circuit by phase shifters. Neighbouring elements were decoupled by overlap, resulting in a total array size of 19 x 26 cm. This design was chosen to cover more than half of the mini pig chest (about 50cm) and to simplify the placement of the coil in the experimental setting. The 4 x 4 array is made from flexible printed circuit board, "baked" into PE foam in order to obtain high flexibility.

A single tuned quadrature ^{13}C birdcage coil (Rapid Biomedical, Rimpar, Germany) with an inner diameter of 35 cm and a length of 36 cm was used as TX resonator. It contains no RF

shield but, as the RX array, includes ^{1}H traps for allowing ^{1}H imaging with the body coil. It is actively decoupled by PIN diodes in each leg.

2.2 MR experiments

MR experiments were conducted with a clinical 3T GE scanner (Excite HDx GE Healthcare, USA), using the scanner body coil for proton imaging. For ^{13}C imaging a volumetric TX birdcage coil (Rapid Biomedical, Rimpar, Germany) was used together with the 16-channel RX surface coil previously described.

Coil performance was assessed using a homogenous cylindrical acetate phantom of dimensions 2 cm x 17 cm (diameter x length) and containing 8.5 g [1-^{13}C]acetate, 70 ml H_2O and 0.5 mmol Dotarem. The phantom simulating the mini pig filling factor was placed with its axis perpendicular to the surface coil plane and perpendicular to the birdcage longitudinal axis. The cylinder was inserted between two cubic phantoms 15 x 15 x 30 cm^3 (2.4 g/l NaCl) to mimic the coil load induced by a mini pig.

Phantom ^{13}C acquisition was performed using an “elliptic FIDCSI” sequence with the following parameters: axial plane, FOV 210 mm, 20 x 20 matrix with reduced k-space sampling (208 phase encoding steps), 1024 spectral points, bandwidth 5000 Hz, slice thickness 3 cm, FA 30°, TR 3000 ms. Phantom acquisition was conducted as well with the birdcage as a TX/RX coil as with the birdcage as TX coil and the 16-channel coil in RX mode.

For each channel the 20 x 20 matrix was interpolated onto a 100 x 100 FIDs matrix by 2D FFT spatial decoding, each FID consisting of 1024 points. The SNR profile of the channel k was obtained as:

$$SNR_k(i,j) = \frac{S_k(i,j)}{\sigma_k(i,j)} \qquad \text{for k = 1,…,16} \qquad (1)$$

where $S_k(i,j)$ is the mean of absolute values of the first 15 points of the FID at the i-th, j-th location of the CSI and σk is the standard deviation of the last 256 points of the same FID, where only noise is present.

The global FIDs were obtained with the phased and weighted coil combination method [13]. The global SNR map was computed as previously described for single channels. Single SNR profile and global SNR map were extracted at the center of the acetate phantom.

Animal studies were performed on six healthy male mini pigs (body weight 25 ± 3 kg). The animal was placed inside the birdcage coil in right decubitus position, with the birdcage coil center corresponding to the pig heart. The 16-channel coil was placed next to the chest of the pig with the center of the coil in correspondence to the pig heart (Fig. 2).

Mini pigs were were fasted overnight (12–16 h) and maintained in deep sedation with a continuous infusion of Propofol (2 mg/kg/h, i.v.) and left in spontaneous breathing while monitoring the main living parameters (blood oxygenation, heart rate). A catheter was introduced into a vein of each ear for tracer injection, drugs and solution infusion. This protocol was approved by the Italian Ministry of Health and was in accordance with Italian law (DL.116, 27 January 1992).

Large doses (350 µl) of [1-^{13}C]pyruvate were formulated with concentration values of: [^{13}C] = 14 M, [OX063] = 15 mM and [Gd3+] = 1 mM. A DNP HyperSense (Oxford Instruments, UK). Polariser was used in combination with a three-step procedure described in [14]. The sample was dissolved in 10 ml of dissolution medium (0.27 mM Na2EDTA in MQ water), the final formulation was obtained by mixing with a buffer solution (200 Trizma, 0.4 mM NaOH in MQ water) externally of the HyperSense, to get a final [1-^{13}C]pyruvate concentration of 230 mM. The dissolved hyperpolarized solution was characterized by a temperature of 37 ± 2°C and 7.6 pH, and was close to isotonic. Then 20 ml of hyperpolarized [1-^{13}C]pyruvate solution were manually injected in a bolus of about 10 s into the right ear vein of the mini pig (effective injected dose = 0.13 mmol/kg body weight); 1 ml was simultaneously transferred to a 1.05 T spectrometer (Bruker BioSpin GmbH, Germany) for T1 relaxation time and liquid-state polarization assessment as reported in [14].

Proton imaging acquisition included short axis views covering the entire LV by a 2D TOF FSPGR sequence, ECG triggered, with TR = 16.6 ms, TE = 2.7 ms, FOV = 30 x 30 cm^2, matrix 288 x 192, slice thickness 4 mm , number of slices 24.

To cover all the LV allowing segmental analysis ^{13}C 3D imaging was performed with a stack of axial plane single-shot spiral trajectory with a FOV of 30 cm, a nominal resolution of 8 mm and a duration of 42 ms using the maximal gradient strength of 40 mT/m and maximal slew rate of 150 T/m of the system. A single time step with seven echo time shifts and twelve phase encoding steps in z-direction was acquired over a FOV of 10 cm in the z-direction. A multiband pulse was used for the excitation, to acquire the metabolites lactate and bicarbonate with a higher flip angle (15°) than pyruvate [15], [16]. Additionally, FIDs of the whole slice were recorded during the acquisition, used for the IDEAL reconstruction and for

inspection of the signal development during the acquisition. Sequence was prescribed following the same short axis orientation defined in the anatomical images. Measurement was started 18 s after injection, at the expected bolus maximum [17]. The data was reconstructed onto a 64 x 64 x 60 grid.

To assess signal distribution on LV wall, three representative SA planes (basal, median and apical) were selected using anatomical images as reference. LV segments were manually defined following the AHA standardized segmentation [18] and the average value of the signal in each of the 16 segments was recorded. AHA model was designed to obtain segments with the same volume. Images were analyzed using the MIPAV software (v 7.1.0, NIH, Bethesda, MD, USA) [19]. Segmental value variations were expressed as percent deviation from the global value obtained by averaging signal values in all segments.

3 Results

The 16-channel surface coil was tuned and matched manually, achieving an S11 (reflection coefficients) and an S12 (transmission coefficient) of better than -20 dB. Average S11 of all RX elements was -22 dB. Ratio of unloaded to loaded Q was 135/98 = 1.4.

Mean S12 of neighbouring elements of the array was -17 dB. The worst S12 of non-neighbouring elements of -8.6 dB was compensated for by the preamplifier decoupling. The sufficient functioning of this decoupling is shown in the noise correlation which was obtained by a noise scan (max 40%, mean 27%, min 10%).

Fig. 3 reports the SNR profiles for each channel evaluated on phantom. The main contribution to the signal was provided by four channels (#6, #7, #10, #11) at the center of the coil in correspondence with the location of the (small) phantom, while contribution of the other channels was negligible.

The sensitivity of the 16-channel coil decreases with the distance as shown in Fig. 4, in which the SNR profile of the combined signal of all channels is reported. For comparison, the SNR profile evaluated with the birdcage coil in TX/RX mode is shown as well. The setup with the birdcage coil permits a more homogeneous image of the entire heart, but losing SNR compared to 16-channel surface coil.

Fig. 5 shows triplanar maps of hyperpolarized [1-^{13}C] pyruvate, lactate and bicarbonate of a pig heart using the 16-channel surface coil. The colour scale represents normalized intensity values of metabolite signals in logarithmic scale. As expected, the signal decreases with the distance of the coil to the chest wall.

Fig. 6(a) and Fig. 6(b) represent the percent variation of signal in LV segments for lactate and bicarbonate in the six imaged mini pigs, respectively. Measured signal deviations were generally consistent throughout the experiments. A longitudinal pattern across the long axis of the LV was well visible. Positive deviations (i.e., signal values higher than average global LV value) were detected in the anterior wall in all slices (segments 1, 7, 13) and in the anterior septum in medium and apical slices (segments 8, 14). A consistent drop of the signal was found in the inferior and lateral-inferior walls (segments 4, 5, 10, 11, 15). Signal in the lateral wall was strongly reduced in the apical slice (segment 16) while in basal and middle slices there was a consistent reduction in some experiments (segments 6 and 12).

Statistical analysis performed by repeated measures analysis of variance (ANOVA) with Scheffè test revealed a significant difference between segments (F-ratio = 7.64, $P < 0.001$). A significant difference was detected between segments 1 vs 16, 4 vs 5-7, 7 vs 11-16, and 8 vs 16 as shown in Fig. 6(a). For bicarbonate signal, a significant difference between segments was detected as well (F-ratio = 3.77, $P = 0.001$). A significant difference was detected between segments 1 vs 3-4, 3 vs 7-13, 4 and 7-13 as shown in Fig. 6.(b).

4 Discussion

In most hyperpolarized ^{13}C heart studies the region of interest is identified with the LV wall, as most of the heart pathologies are related to regional dysfunctions of this region. A typical example is coronary stenosis or occlusion, that leads to a perfusion defect in some LV wall segments, depending on the affected coronary vessel [20]. A standardized LV wall segmentation [18] was proposed by the AHA, which is commonly adopted in clinical and physiological studies. Hence, imaging techniques applied in cardiac studies should provide a uniform sensitivity in the whole LV wall, to avoid variations due to artefacts of segmental signals related to the segment position in LV. On the other hand, the sensitivity of the imaging technique exploiting hyperpolarized agents enriched in ^{13}C should be high enough to detect the signal related to derivate metabolites, which in certain cases could be low due to the reduced flux of conversion [21]. The design of the RF coil configuration to be used in cardiac ^{13}C experiments should take into account both these aspects. This is a challenging task, as a single channel of a multiple channel surface coil provides a high SNR close to the coil surface but a non-uniform sensitivity in depth, while volumetric coils (such as birdcages) provide a uniform sensitivity over the FOV paying in SNR. In this study, we assess the performance of a flexible 16-channel phased array coil to be used in mini pig heart studies, assessing both SNR and signal uniformity by phantom and animal experiments.

In surface coil characterization the ratio of unloaded to loaded Q = 1.4 displays the coil noise dominance. This effect is due to the low frequency of ^{13}C combined with the small coil element size of a multi-channel array while having additional safety measures such as fuses and ^{1}H traps, ensuring patient safety for ^{13}C and for ^{1}H imaging with the body coil.

As shown in Fig. 3, the contribution of coil channels to signal formation in the phantom experiment was concentrated in four channels at the middle of the coil, where the phantom was placed. Since the phantom was small with respect to the coil area, the contribution of peripheral channels was negligible. The global SNR profile (Fig. 4) shows the typical pattern of a surface coil, with a rapid decrease of the SNR with the depth. The comparison with the SNR profile obtained by the birdcage coil used in both transmission and receive mode demonstrates the gain in SNR obtained by the 16-channel coil at a depth below 6 cm. The maximum depth with a reasonable SNR seems to be about 7-8 cm. This depth may be adequate for mini pig LV imaging as in the present study.

In-vivo experiments showed a good metabolite signal in the left ventricular wall, especially in regions nearest to the coil (Fig. 5). The flexible design of the coil allowed detection of signal also in the inferior LV wall, which is a more remote region with respect to the coil surface.

As shown in Fig. 6 for segmental lactate signal, the pattern of signal intensity in the LV segments was reproducible among experiments. A significant drop in the signal was demonstrated in the inferior wall in basal, median and apical slices (segments 4-5, 10-11, 15-16 in AHA model). The maximum signal was measured in the anterior and antero-septal regions (segments 1-2, 7-8, 13-14). The same pattern was detected in bicarbonate signal segmental distribution, although the bicarbonate signal was more difficult to analyze due to the lower intensity. Differences between segments were statistically significant for both lactate and bicarbonate.

The proposed configuration (16-channel flexible surface coil in RX mode and volumetric birdcage coil in TX mode) provided a good signal quality over the whole LV, allowing visualization of the heart metabolism in all LV segments. However, the signal intensity assessed on a normal pig model was significantly different among LV segments. Hence, assessing segmental signal changes may be difficult as variations induced by coil geometry may mask “true” variations induced by physiological changes in LV wall. In principle, it may be possible to correct measurements using a “segmental map” of systematic variations assessed in a normal model [22]. However, an optimized phased array coil configuration

able to provide a near-uniform sensitivity over the FOV would be desirable, such as the two-fold phased array coil with an anterior and a posterior array currently used in heart imaging in clinical practice.

The present study was limited to healthy animals in fasting state, with the objective to have a homogenous concentration of the tracer in the heart to evaluated the homogeneity of the signal acquired by the 16-channels coil. The MR acquisition sequence developed for the study allowed effective 3D heart imaging, but was not designed to monitor the time course of metabolites during the acquisition. Although pre-clinical studies were not yet performed, we would expect that the 16-channel coil could be useful in several protocols. Heart diseases involving the whole LV wall could be better investigated thanks to the higher SNR provided by the coil, as in tachycardia-induced dilated cardiomyopathy studies [23]. Other forms of metabolic heart diseases, such as diabetic cardiomyopathy and Anderson-Fabry disease could benefit from the proposed technology as well [24]. Investigation of the normal cardiac metabolism may represent another important field of application [24]. Heart metabolism could be modulated by infusion of glucose manipulating the metabolic state of the animal towards a fed state following an overnight fast, providing important physiological information [25]. However, following of glucose induced changes would require the design of fast acquisition MR sequences optimized for multi-channels coils [26]. Finally, the 16-channel surface coil in RX mode could be the solution of choice for studying the downstream metabolites of other ^{13}C-enriched molecules, other than pyruvate, for which the SNR could be non-favorable. Recent work on ^{13}C-acetate [21] and ^{13}C-butyrate [27], used as a metabolic probe for short-chain fatty acid metabolism, demonstrated several limitations arising mainly from the low fluxes of conversion and from the low SNR [21] and initial low level of polarization [27]. Further limitations could be recognized in the study. Full 3D covering of the heart was obtained using a 3D sequence with high resolution allowing detailed segmental analysis. However the acquisition of pig images with birdcage only configuration wasn’t possible with this sequence due to the low sensitivity of the coil. For this reason the acquisition sequence using in phantom imaging was slightly different in respect to the one used in pig experiments.

5 Conclusions

A significant improvement of SNR in LV wall near the coil surface could be provided by the coil configuration hereby described, while the drastic reduction of signal in the inferior wall

should discourage the use of the coil in segmental assessment of metabolite distribution in the LV.

References

[1] J. H. Ardenkjaer-Larsen, B. Fridlund, A. Gram, G. Hansson, L. Hansson, M. H. Lerche, R. Servin, M. Thaning, and K. Golman, “Increase in signal-to-noise ratio of > 10,000 times in liquid-state NMR,” *Proc. Natl. Acad. Sci. U. S. A.*, 100: 10158-10163, 2003.

[2] M. F. Santarelli, V. Positano, G. Giovannetti, F. Frijia, L. Menichetti, J.-H. Ardenkjaer-Larsen, D. De Marchi, V. Lionetti, G. Aquaro, M. Lombardi, and L. Landini, “How the signal-to-noise ratio influences hyperpolarized 13C dynamic MRS data fitting and parameter estimation,” *NMR Biomed.*, 25: 925-934, 2012.

[3] K. Golman, L. E. Olsson, O. Axelsson, S. Månsson, M. Karlsson, and J. S. Petersson, “Molecular imaging using hyperpolarized 13C,” *Br. J. Radiol.*, 76: S118-S127, 2003.

[4] Y. F. Yen, S. J. Kohler, A. P. Chen, J. Tropp, R. Bok, J. Wolber, M. J. Albers, K. A. Gram, M. L. Zierhut, I. Park, V. Zhang, S. Hu, S. J. Nelson, D. B. Vigneron, J. Kurhanewicz, H. A. Dirven, and R. E. Hurd, “Imaging considerations for in vivo 13C metabolic mapping using hyperpolarized 13C-pyruvate,” *Magn. Reson. Med.*, 62: 1-10, 2009.

[5] S. E. Day, M. I. Kettunen, F. A. Gallagher, D. E. Hu, M. Lerche, J. Wolber, K. Golman, J. H. Ardenkjaer-Larsen, and K. M. Brindle, “Detecting tumor response to treatment using hyperpolarized 13C magnetic resonance imaging and spectroscopy,” *Nat. Med.*, 13: 1382-1387, 2007.

[6] K. Golman, J. S. Petersson, P. Magnusson, E. Johansson, P. Akeson, C. M. Chai, G. Hansson, and S. Månsson, “Cardiac metabolism measured noninvasively by hyperpolarized 13C MRI,” *Magn. Reson. Med.,* 59: 1005-1013, 2008.

[7] G. Giovannetti, F. Frijia, L. Menichetti, M. Milanesi, J. H. Ardenkjaer-Larsen, D. De Marchi, V. Hartwig, V. Positano, L. Landini, M. Lombardi, and M. F. Santarelli, “Hyperpolarized 13C MRS surface coil: design and signal-to-noise ratio estimation,” *Med. Phys.*, 37: 5361-5369, 2010.

[8] G. Giovannetti, V. Hartwig, F. Frijia, L. Menichetti, V. Positano, J. H. Ardenkjaer-Larsen, V. Lionetti, G. D. Aquaro, D. D. Marchi, A. Flori, L. Landini, M. Lombardi, and M. F. Santarelli, “Hyperpolarized 13C MRS Cardiac Metabolism Studies in Pigs: Comparison Between Surface and Volume Radiofrequency Coils,” *Appl. Magn. Reson.*, 42: 413-428, 2012.

[9] G. Giovannetti, F. Frijia, S. Attanasio, L. Menichetti, V. Hartwig, N. Vanello, J. H. Ardenkjaer-Larsen, D. De Marchi, V. Positano, R. Schulte, L. Landini, M. Lombardi, and M. F. Santarelli, “Magnetic resonance butterfly coils: Design and application for hyperpolarized 13C studies,” *Measurement*, 46: 3282-3290, 2013.

[10] G. Giovannetti, F. Frijia, V. Hartwig, S. Attanasio, L. Menichetti, N. Vanello, V. Positano, J. h. Ardenkjaer-Larsen, V. Lionetti, G. d. Aquaro, D. D. Marchi, R. F. Schulte, F. Wiesinger, L. Landini, M. Lombardi, and M. F. Santarelli, “Design of a quadrature surface coil for hyperpolarized 13C MRS cardiac metabolism studies in pigs,” *Concepts Magn. Reson. Part B Magn. Reson. Eng.*, 43: 69-77, 2013.

[11] W. Dominguez-Viqueira, A. Z. Lau, A. P. Chen, and C. H. Cunningham, “Multichannel receiver coils for improved coverage in cardiac metabolic imaging using prepolarized 13C substrates,” *Magn. Reson. Med.,* 70: 295-300, 2013.

[12] T. Lanz, M. Durst, M. Müller, F. Frijia, G. Giovannetti, L. Menichetti, M. Lombardi, J. H. Ardenkjaer-Larsen, and R. F. Schulte, “A 16 Channel Cardiac Array for Accelerated Hyperpolarised 13C Metabolic Imaging on Pigs at 3T,” *Proc. Intl. Soc. Mag. Reson. Med*., 21: 3947, 2013.

[13] E. G. Larsson, D. Erdogmus, R. Yan, J. C. Principe, and J. R. Fitzsimmons, “SNR-optimality of sum-of-squares reconstruction for phased-array magnetic resonance imaging,” *J. Magn. Reson.,* 163: 121-123, 2003.

[14] A. Flori, F. Frijia, V. Lionetti, J. H. Ardenkjaer-Larsen, V. Positano, G. Giovannetti, R. F. Schulte, F. Wiesinger, F. A. Recchia, L. Landini, M. F. Santarelli, M. Lombardi, and L. Menichetti, “DNP Methods for Cardiac Metabolic Imaging with Hyperpolarized [1-13C]pyruvate Large Dose Injection in Pigs,” *Appl. Magn. Reson.*, 43: 299-310, 2012.

[15] U. Köllisch, R. F. Schulte, M. Durst, J. H. Ardenkjaer-Larsen, F. Frijia, L. Menichetti, M. Lombardi, A. Haase, and F. Wiesinger, “3D Whole-Heart Cardiac Metabolic Imaging with [1- 13 C]pyruvate using IDEAL Spiral CSI,” *Proc. Intl. Soc. Mag. Reson. Med.*, 21: 3923, 2013

[16] P. E. Z. Larson, A. B. Kerr, A. P. Chen, M. S. Lustig, M. L. Zierhut, S. Hu, C. H. Cunningham, J. M. Pauly, J. Kurhanewicz, and D. B. Vigneron, “Multiband excitation pulses for hyperpolarized 13C dynamic chemical-shift imaging,” *J. Magn. Reson.*, 194: 121-127, 2008.

[17] L. Menichetti, F. Frijia, A. Flori, F. Wiesinger, V. Lionetti, G. Giovannetti, G. D. Aquaro, F. A. Recchia, J. H. Ardenkjaer-Larsen, M. F. Santarelli, and M. Lombardi, “Assessment of real-time myocardial uptake and enzymatic conversion of hyperpolarized [1-^{13}C]pyruvate in pigs using slice selective magnetic resonance spectroscopy,” *Contrast Media Mol. Imaging*, 7: 85-94, 2012.

[18] M. D. Cerqueira, N. J. Weissman, V. Dilsizian, A. K. Jacobs, S. Kaul, W. K. Laskey, D. J. Pennell, J. A. Rumberger, T. Ryan, and M. S. Verani, “Standardized myocardial segmentation and nomenclature for tomographic imaging of the heart” *Circulation*, 105: 539-542, 2002.

[19] M. J. McAuliffe, F. M. Lalonde, D. McGarry, W. Gandler, K. Csaky, and B. L. Trus, “Medical Image Processing, Analysis and Visualization in clinical research,” *Proceedings of 14th IEEE Symposium on Computer-Based Medical Systems,* 381-386, 2001.

[20] G. D. Aquaro, F. Frijia, V. Positano, L. Menichetti, M. F. Santarelli, J. H. Ardenkjaer-Larsen, F. Wiesinger, V. Lionetti, S. L. Romano, G. Bianchi, D. Neglia, G. Giovannetti, R. F. Schulte, F. A. Recchia, L. Landini, and M. Lombardi, “3D CMR mapping of metabolism by hyperpolarized 13C-pyruvate in ischemia-reperfusion,” *JACC Cardiovasc. Imaging*, 6: 743–744, 2013.

[21] A. Flori, M. Liserani, F. Frijia, G. Giovannetti, V. Lionetti, V. Casieri, V. Positano, G. D. Aquaro, F. A. Recchia, M. F. Santarelli, L. Landini, J. H. Ardenkjaer-Larsen, and L. Menichetti, “Real-time cardiac metabolism assessed with hyperpolarized [1-13C]acetate in a large-animal model,” *Contrast Media Mol. Imaging*, 10: 194-202, 2015.

[22] V. Positano, A. Pepe, M. F. Santarelli, B. Scattini, D. De Marchi, A. Ramazzotti, G. Forni, C. Borgna-Pignatti, M. E. Lai, M. Midiri, A. Maggio, M. Lombardi, and L. Landini, “Standardized T2* map of normal human heart in vivo to correct T2* segmental artefacts,” *NMR Biomed.*, 20, 6: 578–590, 2007.

[23] M. A. Schroeder, A. Z. Lau, A. P. Chen, Y. Gu, J. Nagendran, J. Barry, X. Hu, J. R. Dyck, D. J. Tyler, K. Clarke, K. A. Connelly, G. A. Wright, and C. H. Cunningham, “Hyperpolarized 13C magnetic resonance reveals early- and late-onset changes to in vivo pyruvate metabolism in the failing heart,” *Eur. J. Heart. Fail.*, 15: 130-140, 2013.

[24] M. A. Schroeder, K. Clarke, S. Neubauer, D. J. Tyler. “Hyperpolarized Magnetic Resonance. A Novel Technique for the In Vivo Assessment of Cardiovascular Disease,” *Circulation*, 124: 1580-1594, 2011.

[25] M. H. Lauritzen, C. Laustsen, S. A. Butt, P. Magnusson, L. V. Søgaard, J. H. Ardenkjær-Larsen, and P. Åkeson, “Enhancing the [13C]bicarbonate signal in cardiac hyperpolarized [1-13C]pyruvate MRS studies by infusion of glucose, insulin and potassium,” *NMR Biomed*., 26: 1496-1500, 2013.

[26] A. Z. Lau , A. P. Chen, N. R. Ghugre, V. Ramanan, W. W. Lam, K. A. Connelly, G. A. Wright, C. H. Cunningham, “Rapid Multislice Imaging of Hyperpolarized 13C Pyruvate and Bicarbonate in the Heart,” *Magn. Reson. Med*., 64: 1323-1331, 2010.

[27] D. R. Ball, B. Rowlands, M. S. Dodd, L. Le Page, V. Ball, C. A. Carr, K. Clarke, and D. J. Tyler, “Hyperpolarized butyrate: a metabolic probe of short chain fatty acid metabolism in the heart,” *Magn. Reson. Med*., 71:1663-1669, 2014.

Figure Captions

Fig. 1. a) Housing of the flexible RX array; b) Disposition of elements on the coil plane; c) electrical circuitry of a single coil element, including tune, match, active and passive detuning, fuse, preamplifier (VV) and cable trap (MWS)

Fig. 2. Experimental setup including the TX birdcage and the RX array on a pig

Fig. 3. SNR profiles of a 2.4 g/l NaCl cylinder phantom inserted between two cubic phantoms with a size of 15 x 15 x 30 cm for each of the 16 channels. Channel disposition illustrated in Fig. 2.d

Fig. 4. Global SNR profile for the RX16-channel surface coil and the TX/RX birdcage coil

Fig. 5. Triplanar views of pyruvate, lactate and bicarbonate on the three main heart axes

Fig. 6. Box-and-whisker plots illustrating segmental variability of the lactate (a) and bicarbonate (b) signal in animal experiments for each segment

a

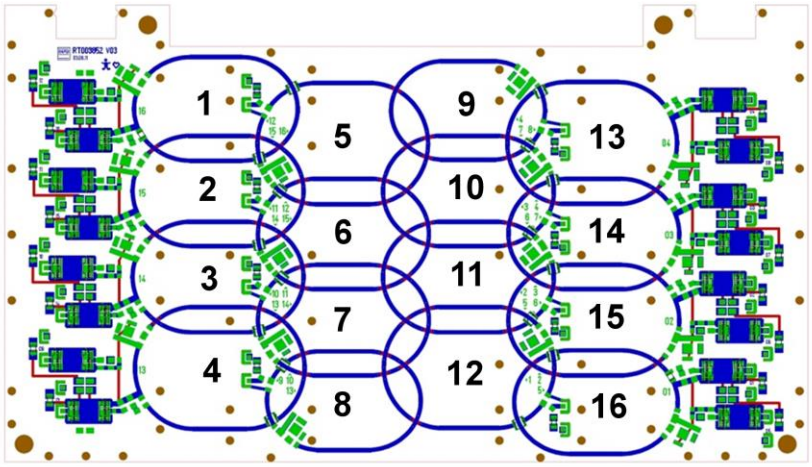

b

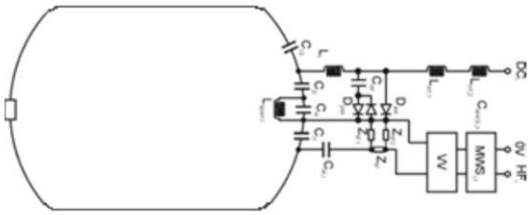

c

Figure 1

Figure 2

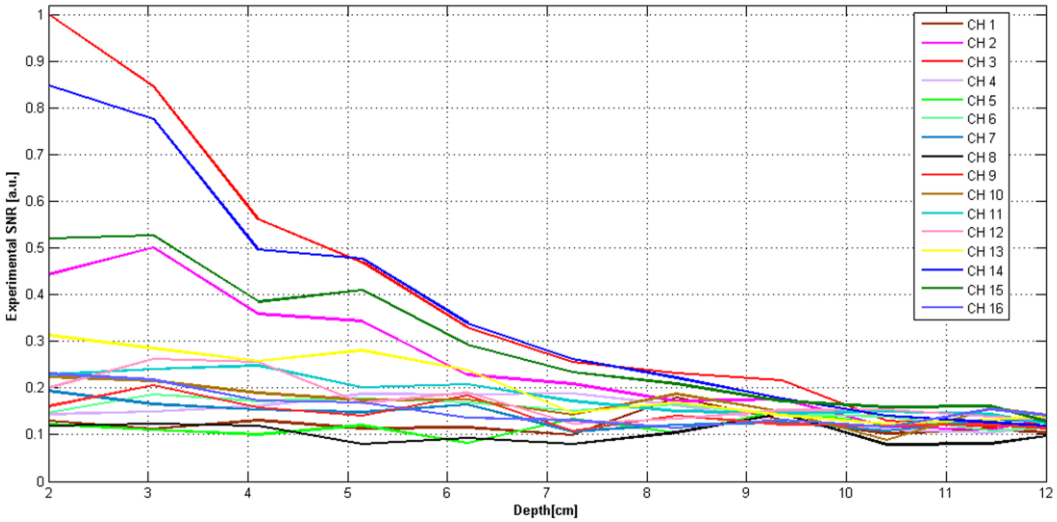
Experimental SNR [a.u.]
Depth[cm]
CH 1
CH 2
CH 3
CH 4
CH 5
CH 6
CH 7
CH 8
CH 9
CH 10
CH 11
CH 12
CH 13
CH 14
CH 15
CH 16

Figure 3

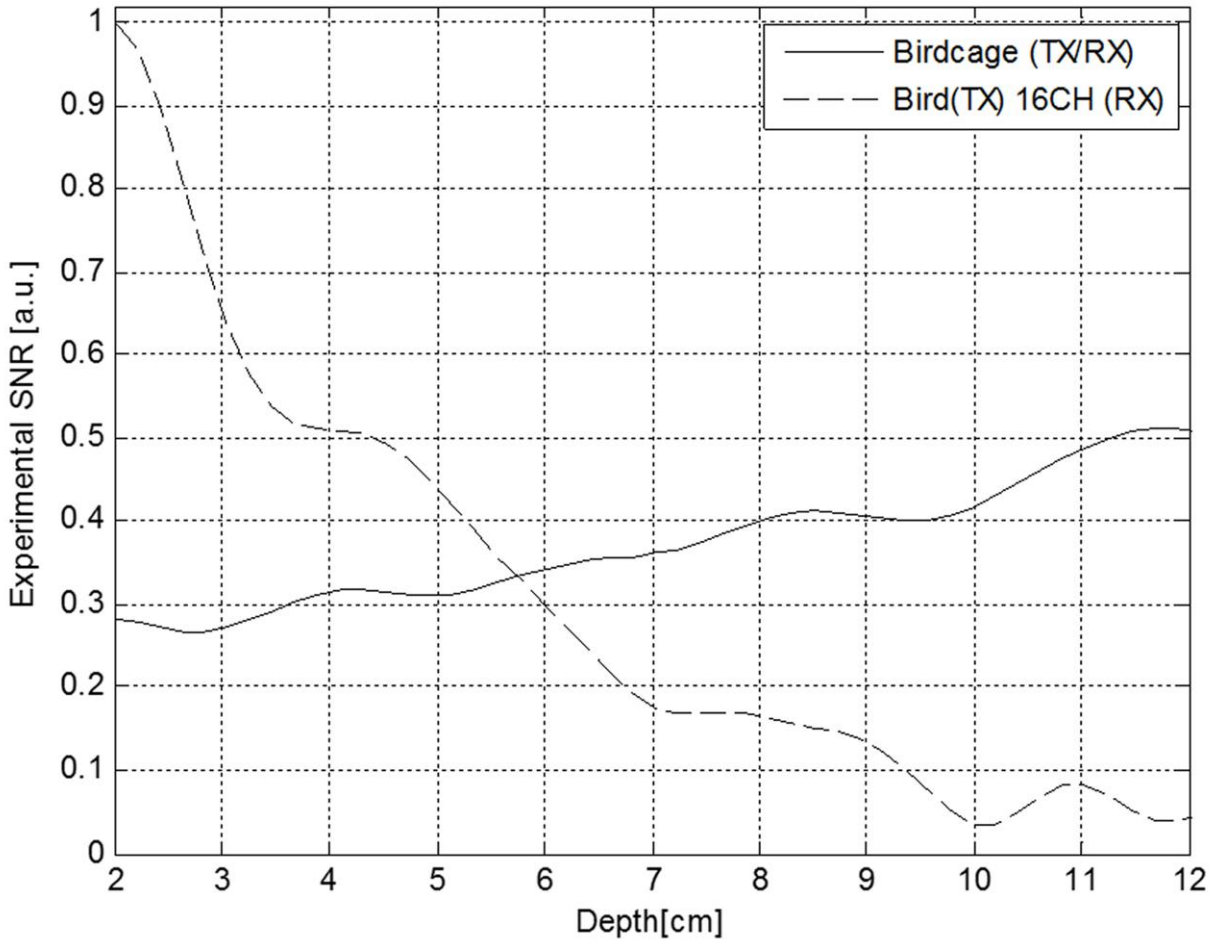
Birdcage (TX/RX)
Bird(TX) 16CH (RX)
Experimental SNR [a.u.]
Depth[cm]
0
0.1
0.2
0.3
0.4
0.5
0.6
0.7
0.8
0.9
1
2
3
4
5
6
7
8
9
10
11
12

Figure 4

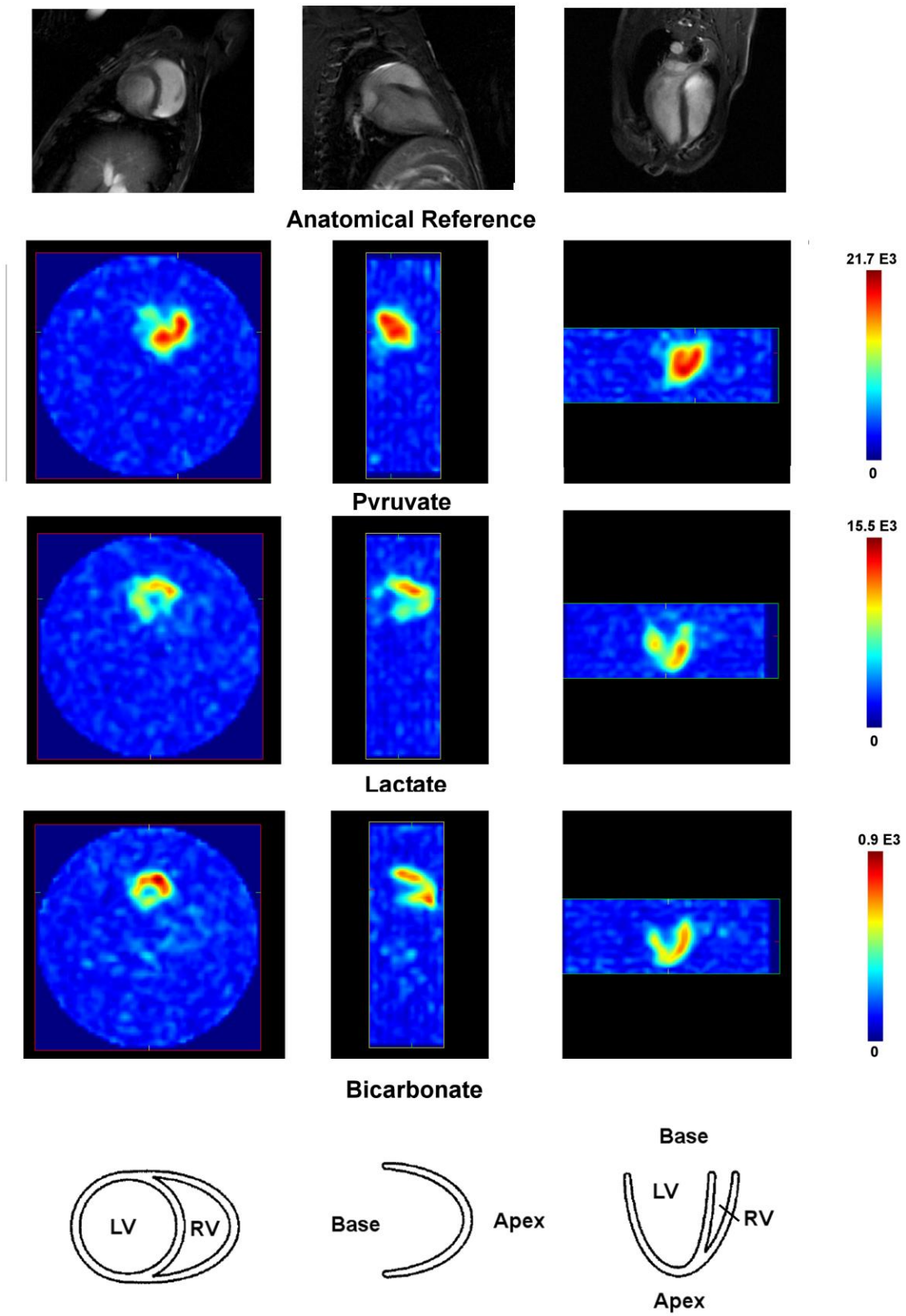
Anatomical Reference
21.7 E3
0
Pvruvate
15.5 E3
0
Lactate
0.9 E3
0
Bicarbonate
LV
RV
Base
Apex
Base
LV
RV
Apex

Figure 5

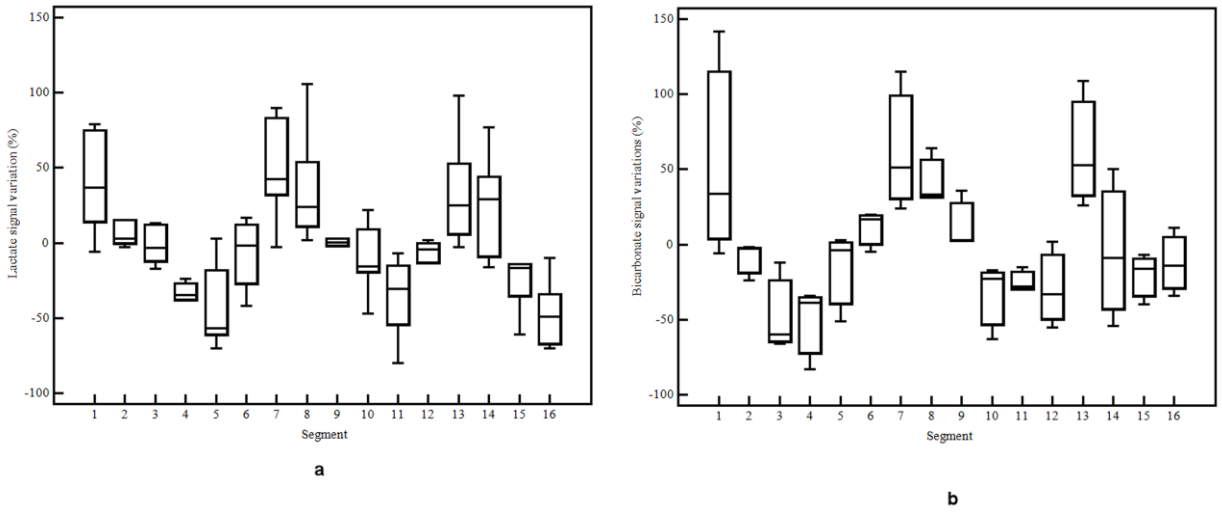
Lactate signal variation (%)
150
100
50
0
-50
-100
1 2 3 4 5 6 7 8 9 10 11 12 13 14 15 16
Segment
a
Bicarbonate signal variations (%)
150
100
50
0
-50
-100
1 2 3 4 5 6 7 8 9 10 11 12 13 14 15 16
Segment
b

Figure 6

Figure 1
Click here to download Figure: Figure 1.tif

a

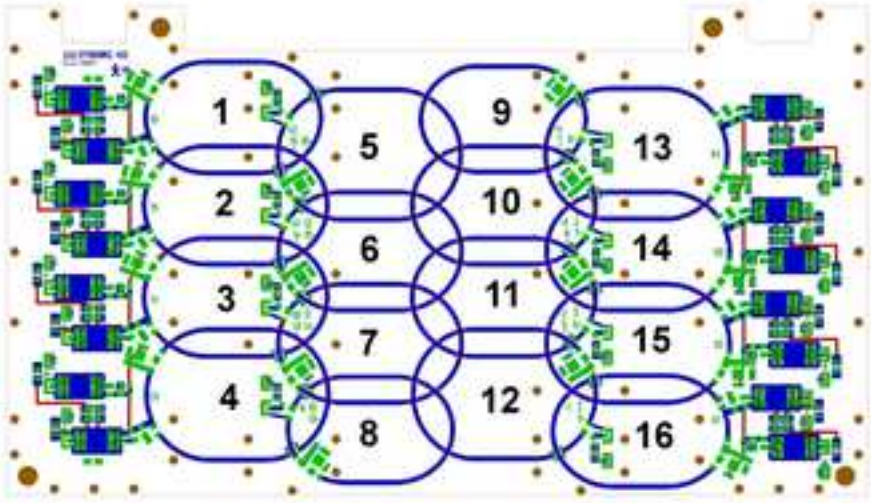

b

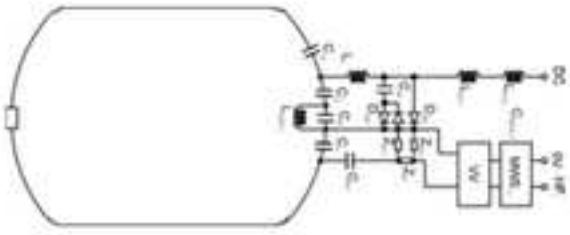

c

Figure 2
Click here to download Figure: Figure2.tif

Figure 3
Click here to download Figure: Figure 3.tif

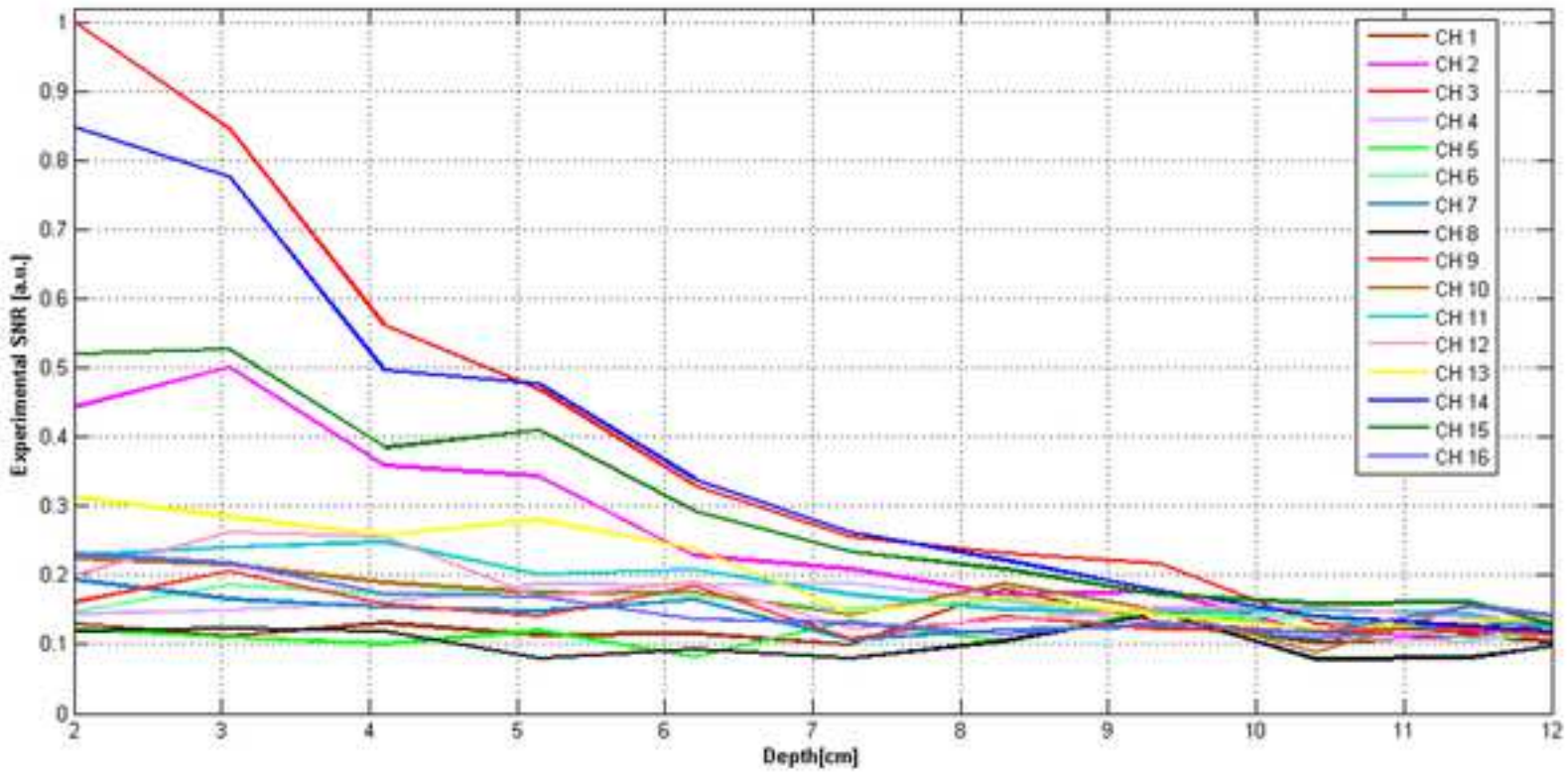

Figure 4
Click here to download Figure: Figure4.tif

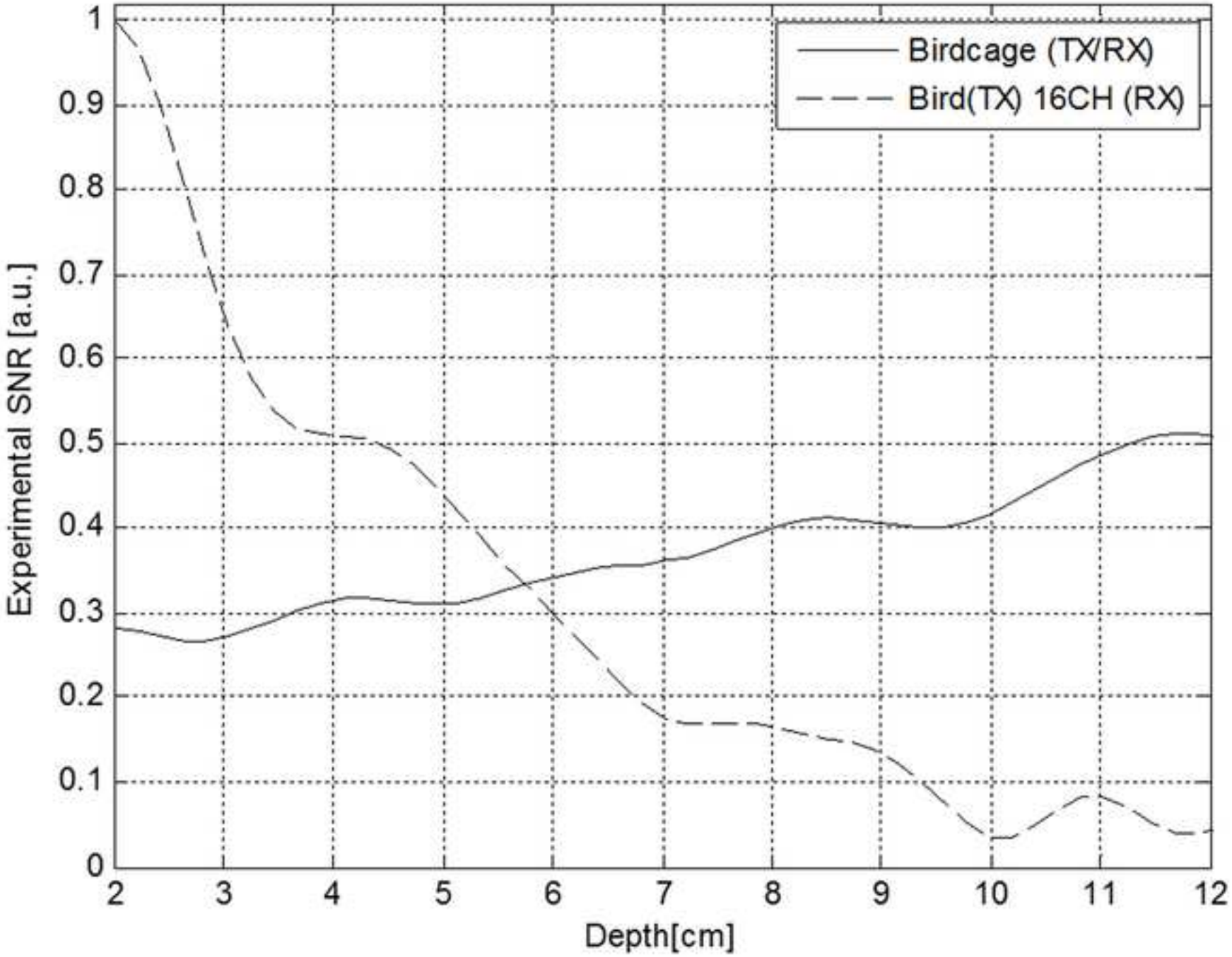

Figure 5
Click here to download Figure: Figure5.tif

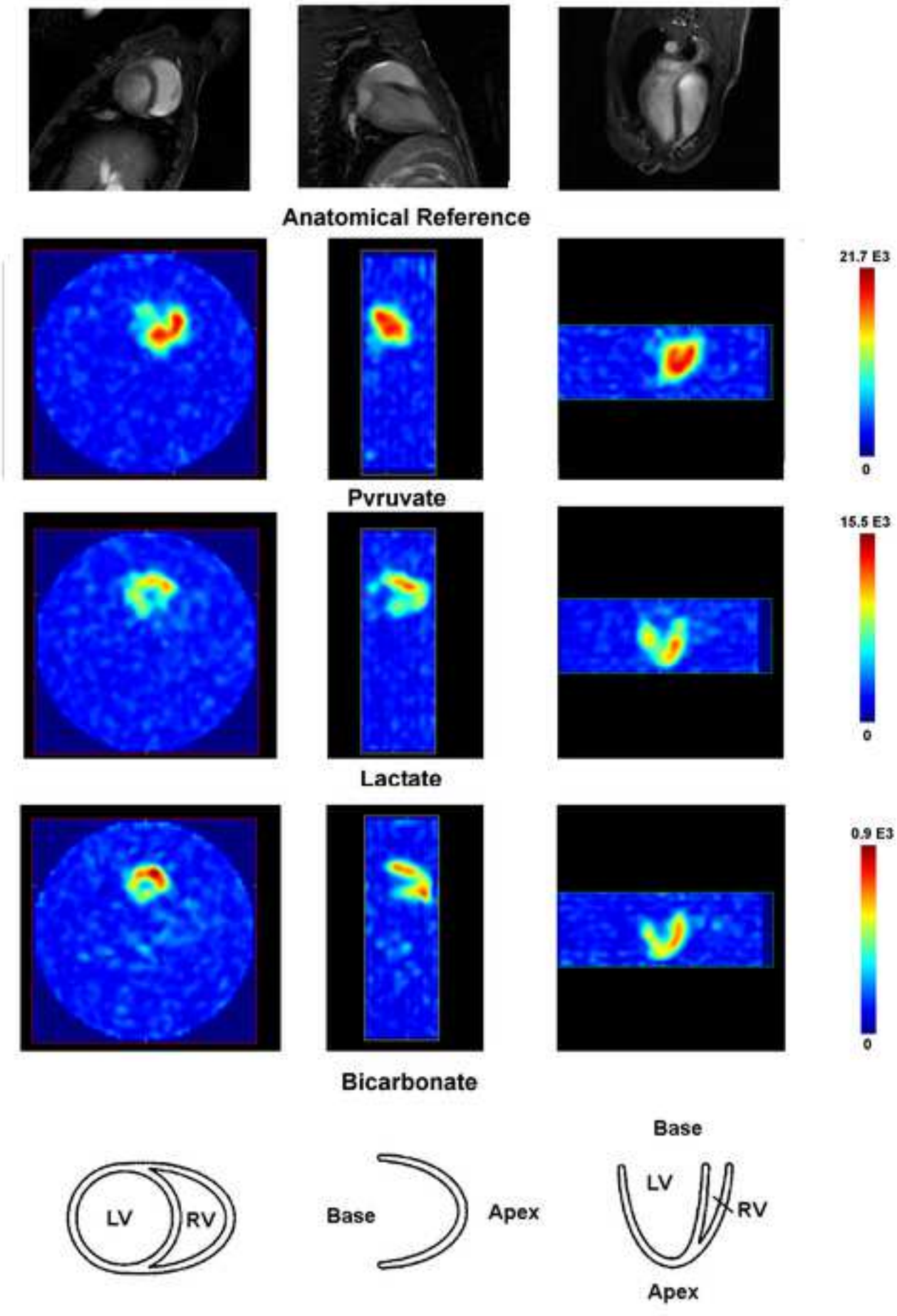

Figure 6
Click here to download Figure: Figure6.tif

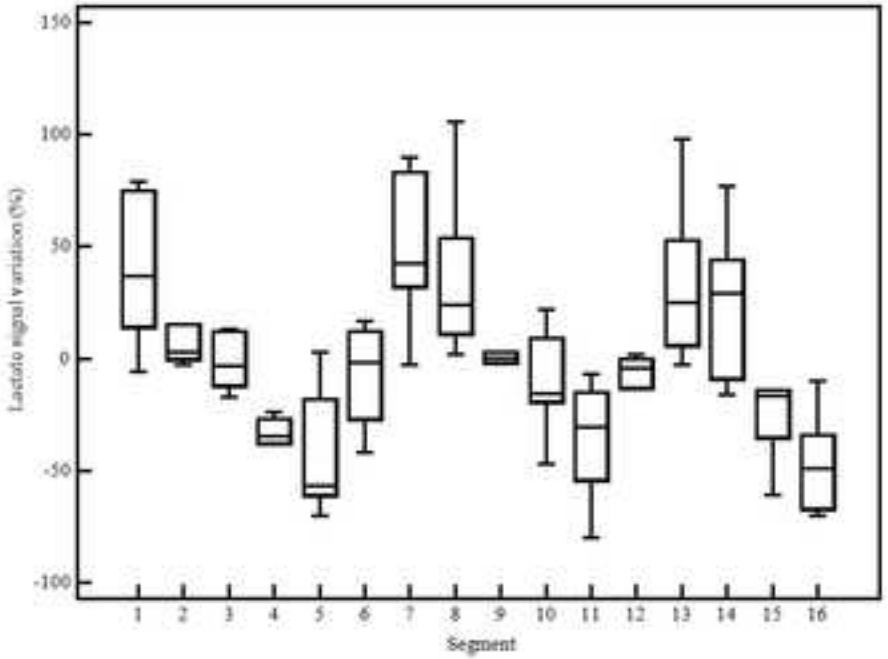

a

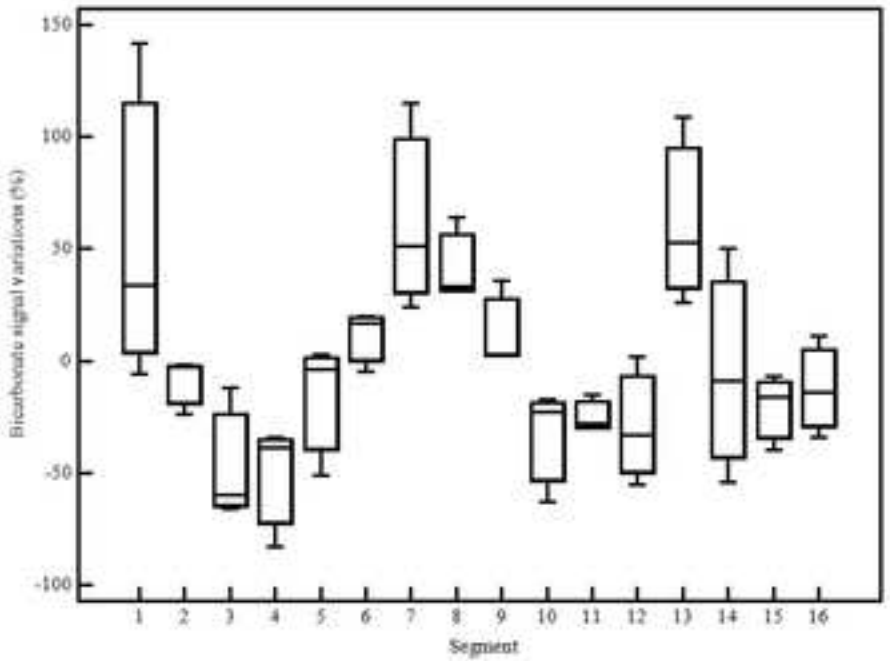

b